

# Using Stable Water Isotope Measurements to Determine Lake Michigan Evaporation Influence on Atmospheric Moisture

Alexandra Meyer<sup>1</sup>, Lisa Welp<sup>1,4</sup>, Thilina Jayarathne<sup>2</sup>, Olivia Salmon<sup>2</sup>, Brian Stirm<sup>3</sup>, Michael Baldwin<sup>1,4</sup>, Paul Shepson<sup>1,2</sup>

<sup>1</sup>Department of Earth, Atmospheric, and Planetary Sciences, Purdue University, <sup>2</sup>Department of Chemistry, Purdue University, <sup>3</sup>Department of Aviation and Transportation Technology, Purdue University, <sup>4</sup>Purdue Climate Change Research Center, Purdue University



## Introduction

- The Great Lakes region provides energy and moisture to fuel seasonal convective storms and lake-effect snow (Sharma, et al. 2018).
- Estimates of the Great Lakes influence downwind have been constructed using water isotopes and the Craig Gordon Model (Equation 1), but there is some uncertainty about how large the kinetic fractionation ( $\epsilon_k$ ) is in this environment.
  - Gat, et al. (1994) found ~5.7-9.5% of the atmospheric water vapor downwind of the lakes is from lake evaporation using  $\epsilon_k = 14.2\text{‰ } \delta^{18}\text{O}$  and  $12.5\text{‰ } \delta\text{D}$  (Lake  $\epsilon_k$ ).
  - Xiao, et al. (2018) found ~7.4% when using the Lake  $\epsilon_k$  and ~16.8% when using the ocean  $\epsilon_k$  parameterization ( $\epsilon_k = 6.2\text{‰ } \delta^{18}\text{O}$  and  $5.5\text{‰ } \delta\text{D}$ ).
- The difference between the two fractionation factors may be partially due to a lake self-influence parameter, based on humidity, turbulence, and where the atmosphere was measured (Xiao, et al. 2018).
- To better constrain downwind Great Lakes influence, aircraft measurements of atmospheric water vapor isotopes around Lake Michigan were made.

## Objectives:

- Measure the gradient of  $\text{H}_2\text{O}_v$  and isotopic values across upwind to downwind lake influence gradients to test the isotopic predictions of the Craig-Gordon model of evaporation.

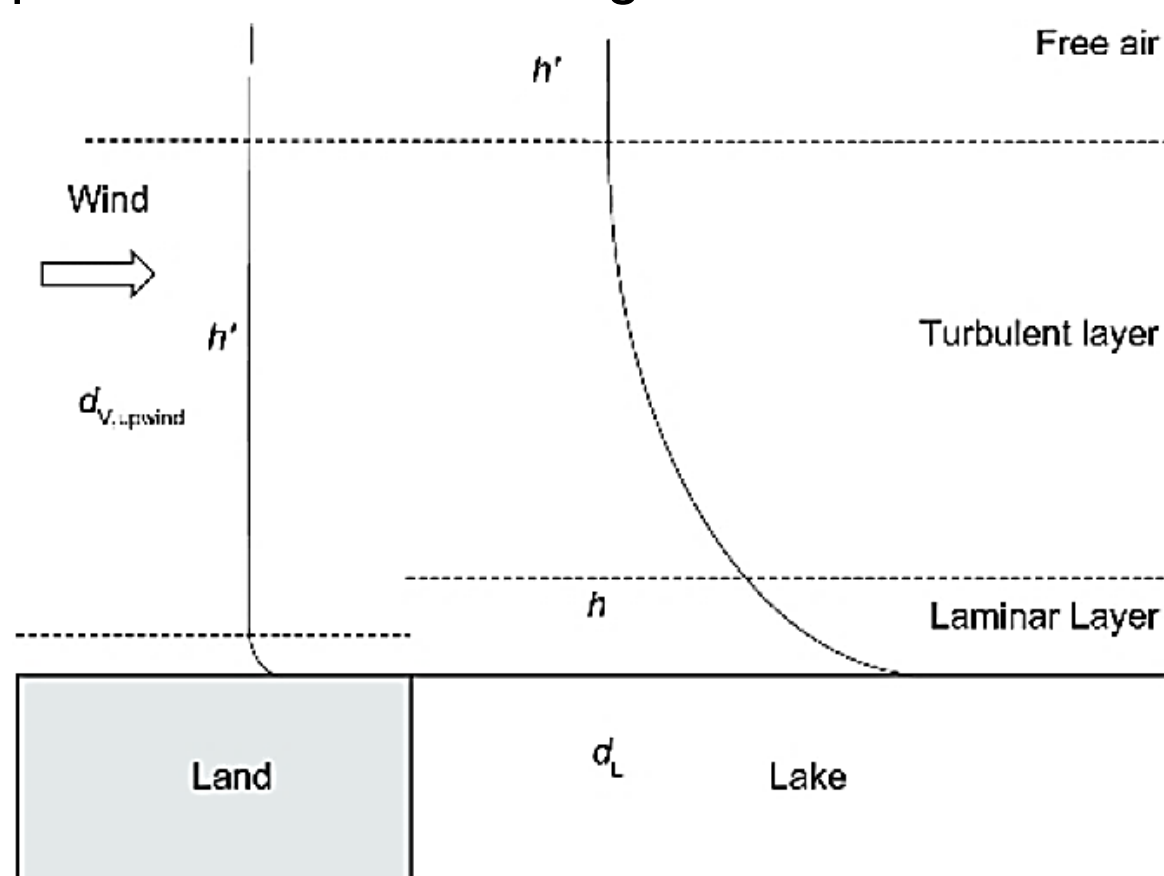


Figure 1. Conceptual diagram of lake influence from Xiao, et al. (2018).

## Materials and Methods

$$\delta_E = \frac{\alpha_{eq}^{-1} \delta_L - h \delta_A - \epsilon^* - \epsilon_k (1-h)}{(1-h) + 10^{-3} (1-h) \epsilon_k}$$

Equation 1. Craig and Gordon Model (Xiao et al. 2016). This equation was created to explain the isotopic composition of evaporation ( $\delta_E$ ) in oceans. Parameters include equilibrium fractionation ( $\alpha_{eq}$ ), the isotopic value of the lake and atmosphere ( $\delta_L$  and  $\delta_A$ ), relative humidity ( $h$ ), and a kinetic fractionation factor ( $\epsilon_k$ ). This equation parameterizes  $\epsilon_k$  as a factor of wind speed.

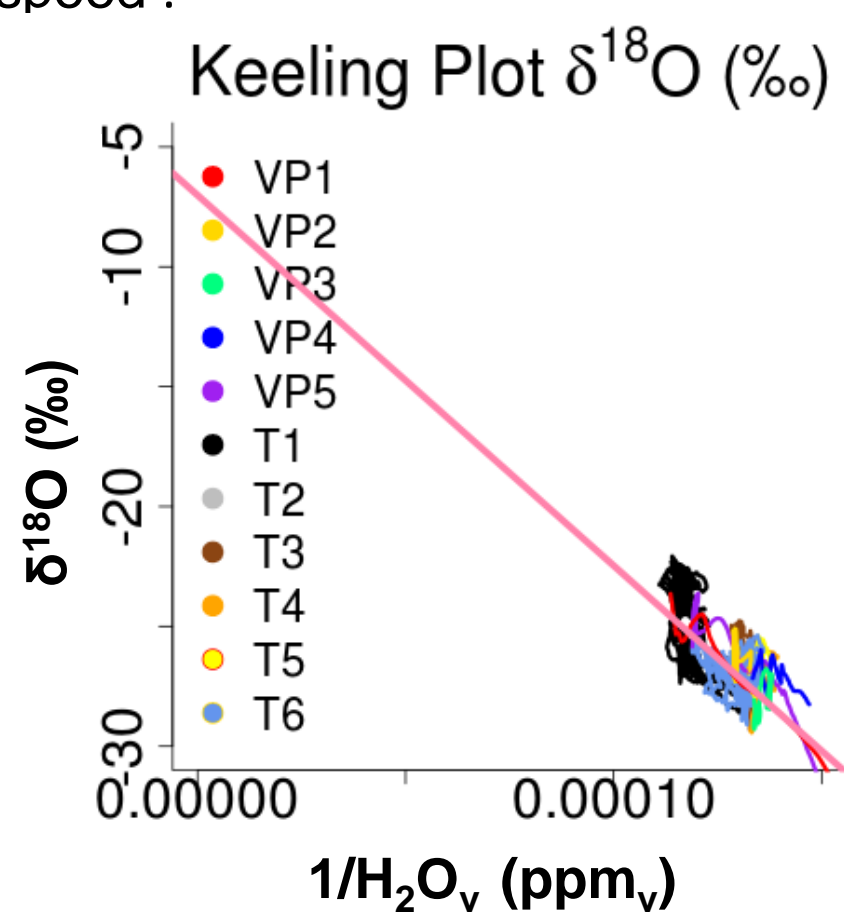


Figure 2. (a) Example Keeling Plot for Flight 4. Keeling Plot intercepts are an estimate of  $\delta_E$  when it is assumed that there are two sources and the upwind value doesn't change significantly over time, and Ordinary Least Squares regression and data screening based on a height 500 m, wind direction, and  $\text{CO}_2$  were used (Pataki et al, 2003).

Flights were completed using the Purdue University Airborne Laboratory for Atmospheric Research (ALAR), a modified Beechcraft Duchess aircraft.

- Best Air Turbulence (BAT) Probe measures winds and temperatures
- Picarro  $\text{CO}_2/\text{CH}_4/\text{H}_2\text{O}$  Cavity Ringdown Spectroscopy analyzer
- Los Gatos Research (LGR) 1 Hz Triple Water Vapor Isotope Off-axis Integrated Cavity Output Spectroscopy analyzer
- Flight plans based on many factors, including weather, safety, and aircraft availability

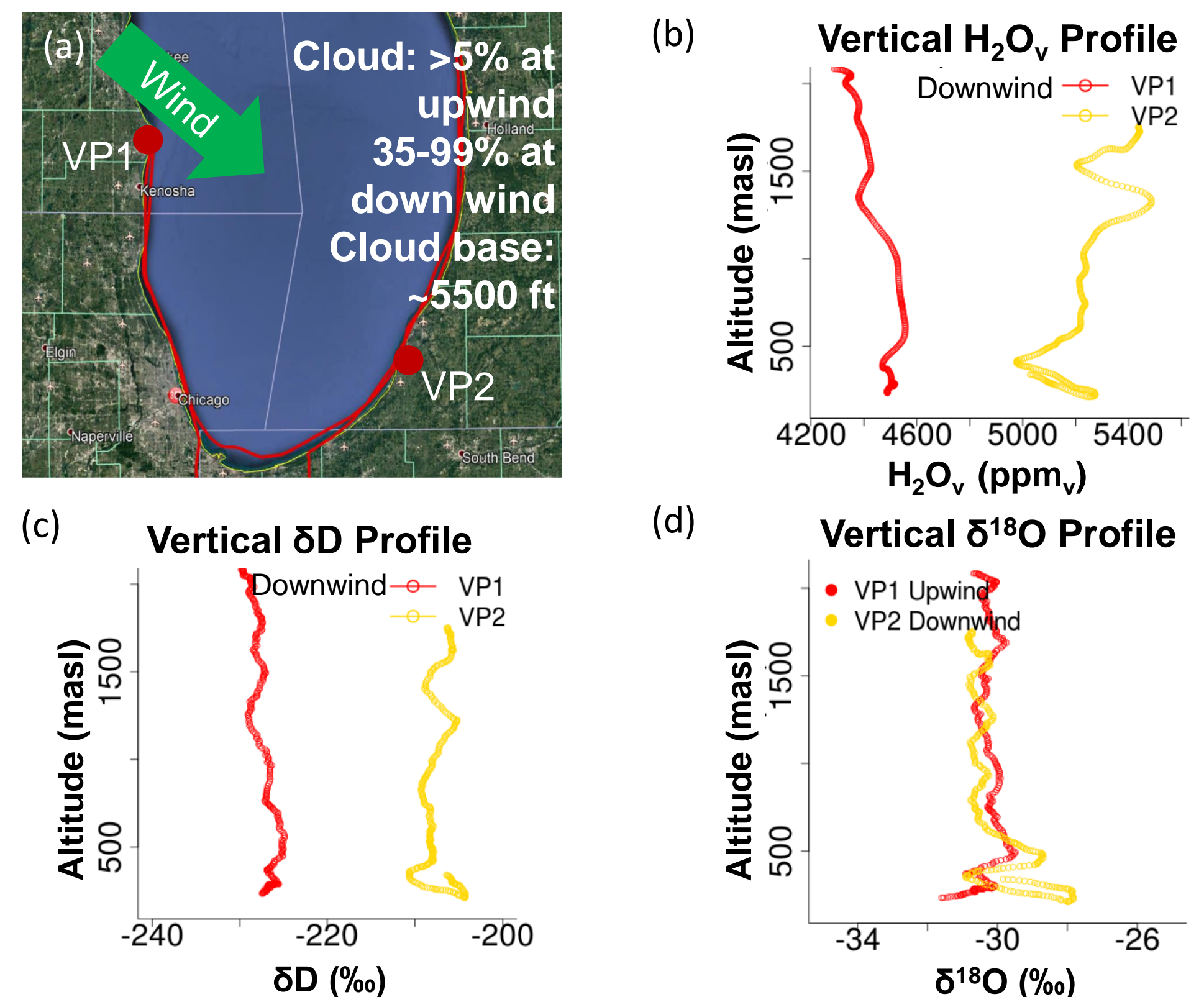


Figure 3. (a) Map of flight 2 path Monday, October 17, 2018. Flight occurred from approximately 11am to 3:30pm local time (EDT). (b) Two Vertical Profiles (VP's) indicate change in (b) water vapor change and (c) deuterium isotopes across the lake. (d). The VP's converge in  $\delta^{18}\text{O}$  space above ~500 masl, but diverge nearer to the surface.

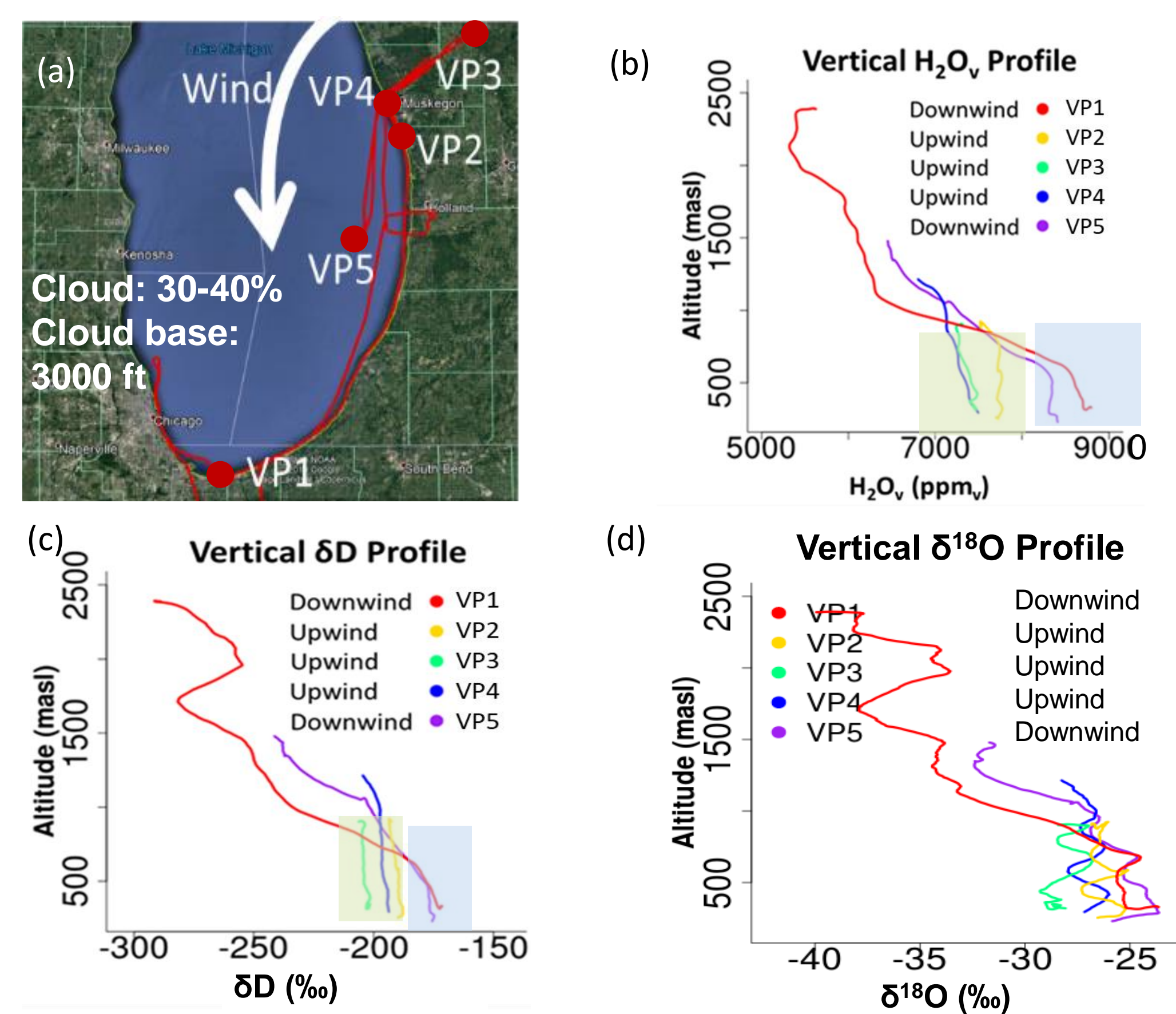


Figure 4. (a) Map of flight 4 path Monday, October 27, 2018. The flight occurred from approximately 12 pm to 5pm local time (EDT). (b) Indicates both horizontal and vertical water vapor gradients. This gradient is also evident in  $\delta\text{D}$  space (c) but is more variable in  $\delta^{18}\text{O}$  space (d).

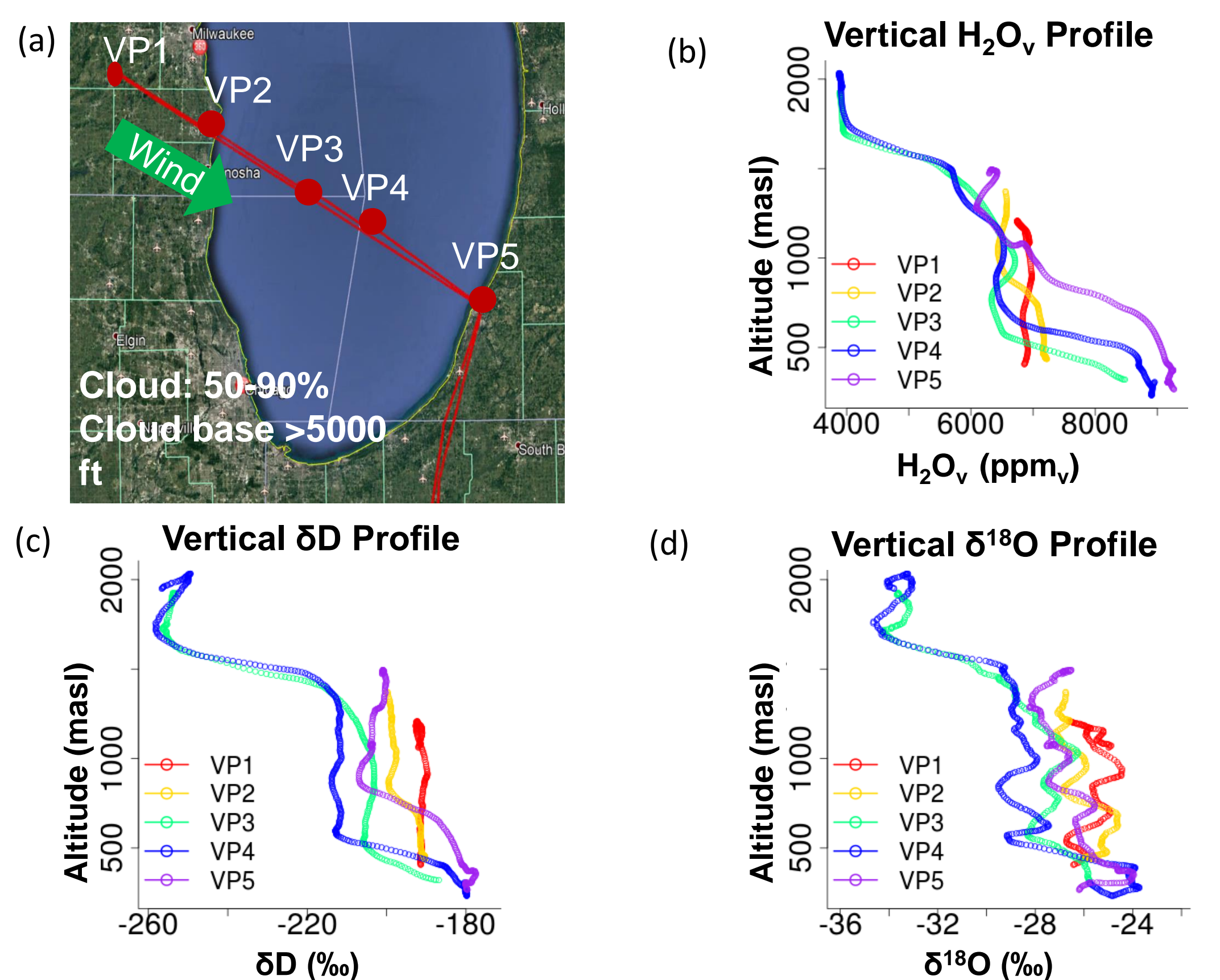


Figure 5. (a) Map of flight path 5 on Monday, October 29, 2018, which occurred from approximately 12pm to 5pm local time (EDT). (b) Water vapor concentration downwind is increased with increasing fetch, indicating both horizontal and vertical water vapor gradients. (c) A similar pattern is seen in  $\delta\text{D}$  space, however again, (d)  $\delta^{18}\text{O}$  profiles are variable.

## Summary and Next Steps

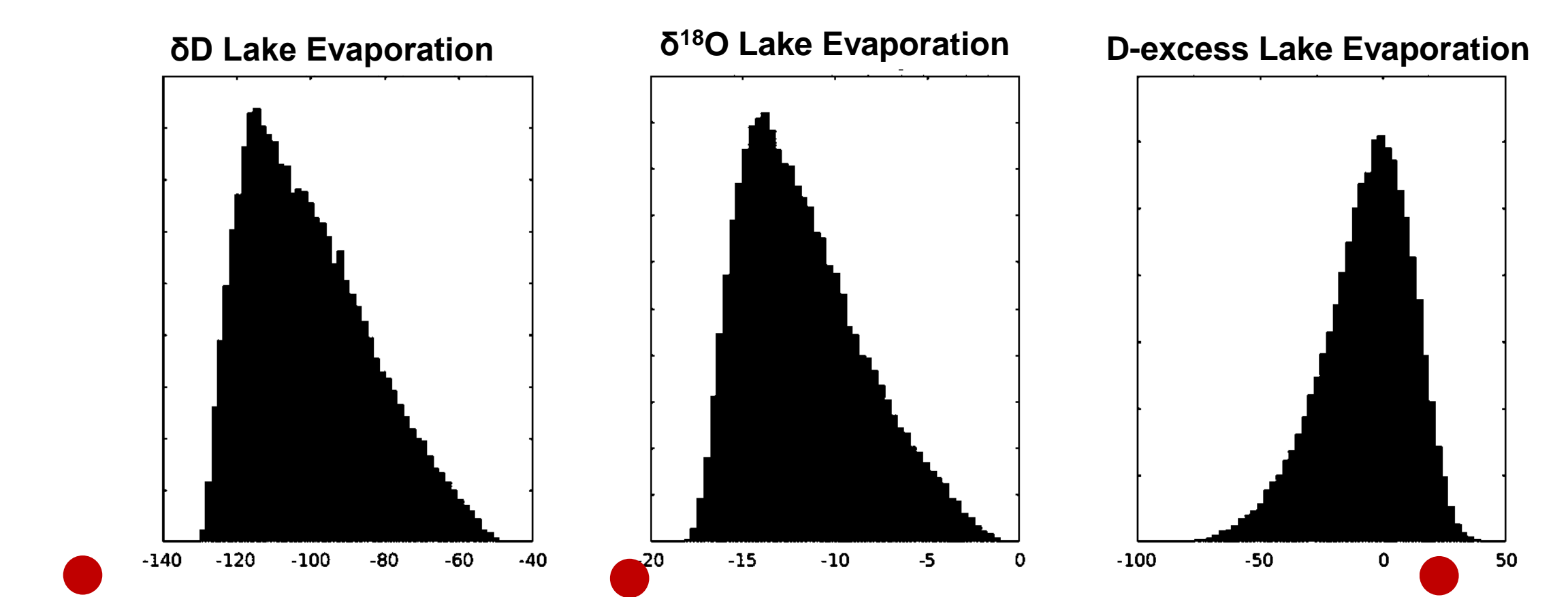
- We see an  $\text{H}_2\text{O}_v$  and deuterium isotope gradient across the lake with increasing fetch. This pattern is more variable but is also seen at the lowest altitudes of  $\delta^{18}\text{O}$  profiles.
- For Flight 4, our CG predictions match our KP results within the Monte Carlo mean  $\pm$  sd. These KP results have a relatively high  $R^2$  of about 0.7.
- Flight 2 and Flight 5 KP values are more depleted than would be expected based on the CG model. Possible explanations include atmospheric mixing, measurement height CG  $\delta_A$  uncertainty, and city/"other" wind influence.
- Future work: Applying a smaller-scale wind direction model to screen data for Keeling Plot applications and exploring observations of  $\delta_A$ , RH, and  $\epsilon_k$ .

## Results

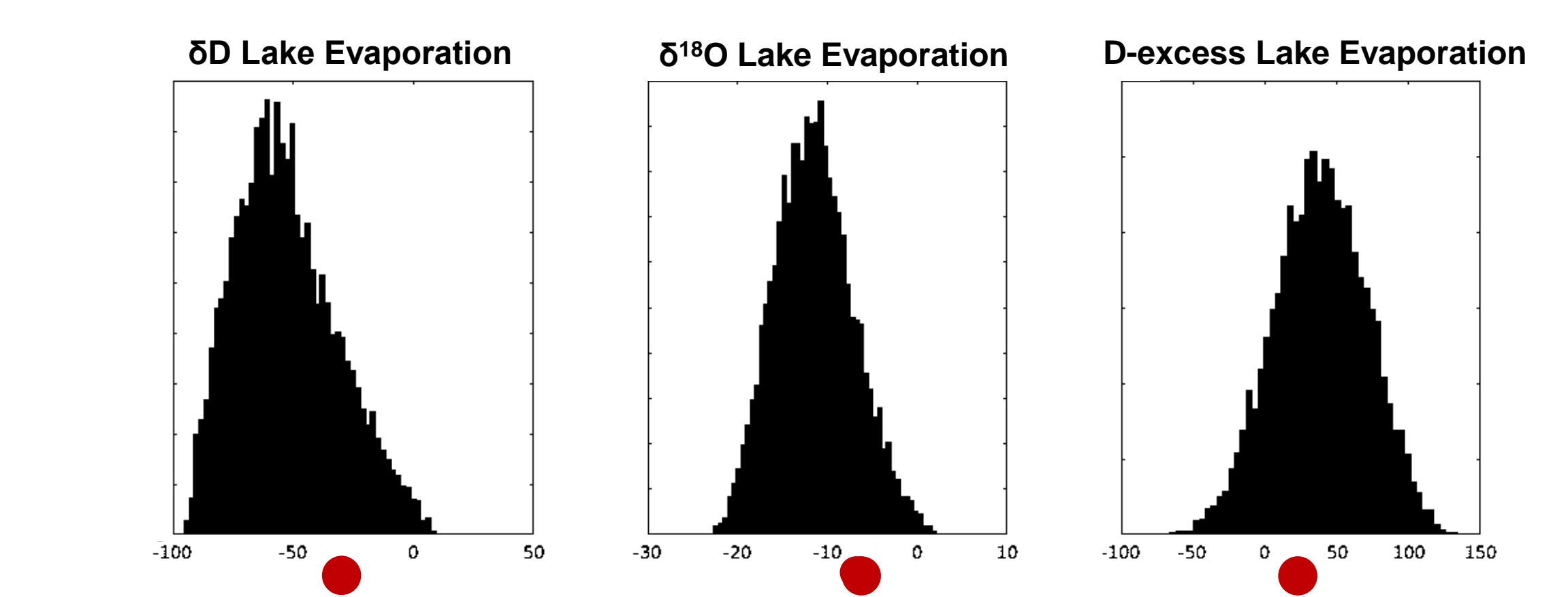
Table 1. Average parameters for flight days (in parentheses) and ranges for Monte Carlo simulations.

Flight Parameters	Flight Parameters		
	Flight 2 10/17	Flight 4 10/27	Flight 5 10/29
Time (UTC)	1600 to 1900	1600 to 2000	1800 to 2000
Air Temperature ( $^{\circ}\text{C}$ )	6.1-8 (6.68)	9.6-10.9 (10.25)	9-11 (9.84)
$\text{H}_2\text{O}$ Temperature ( $^{\circ}\text{C}$ )	(12.20)	(12.41)	(9.53)
RH with respect to air (%)	52-68 (60.29)	63-70 (66.83)	40- 71 (66.4)
RH with respect to lake surface (%)	25-52 (42)	50-65 (58)	40-70 (67.88)
Wind Speed (m/s)	5.9-8.9 (7.63)	3-4 (3.13)	0.70 to 6.2 (3.90)
$\text{H}_2\text{O}$ range (ppm)	4,400 to 5,500	5,500 to 9,000	4,000 to 9,500
$\delta\text{D}$ Atmosphere	-230 to -190 (-225)	-220 to -180 (-200)	-205 to -170 (-190)
$\delta^{18}\text{O}$ Atmosphere	-34 to -25 (-30)	-30 to -24 (-29)	-28 to -22 (-26)
Kinetic Fractionation $\epsilon_k \delta\text{D}$	2-3.5	5-6 (5.54)	5-6 (5.405)
$\epsilon_k \delta^{18}\text{O}$	2.5-4	6-7 (6.28)	6-7 (6.129)
Equilibrium Fractionation $\alpha_{eq} \delta\text{D}$	(1.10230) $\pm$ 0.001	(1.09734) $\pm$ 0.001	(1.09790) $\pm$ 0.001
$\alpha_{eq} \delta^{18}\text{O}$	(1.01103) $\pm$ 0.0001	(1.01068) $\pm$ 0.0001	(1.01072) $\pm$ 0.0001
$\delta_E \delta\text{D}$ CG	-100.48 $\pm$ 16.48	-52.94 $\pm$ 20.95	-100.20 $\pm$ 13.52
$\delta_E \delta\text{D}$ KP intercepts (Adjusted $R^2$ )	-169.1 (0.69)	-36.0 (0.73)	-143.0 (0.86)
$\delta_E \delta^{18}\text{O}$ CG	-11.682 $\pm$ 3.263	-8.219 $\pm$ 3.497	-12.405 $\pm$ 3.925
$\delta_E \delta^{18}\text{O}$ KP intercepts (Adjusted $R^2$ )	-23.98 (0.80)	-7.0 (0.70)	-28.21 (0.14)
d-excess CG	-7.0 $\pm$ 18.1	9.72 $\pm$ 25.46	-0.960 $\pm$ 21.73
d-excess KP	22.9	22.1	82.7

(a) Flight 2



(b) Flight 4



(c) Flight 5

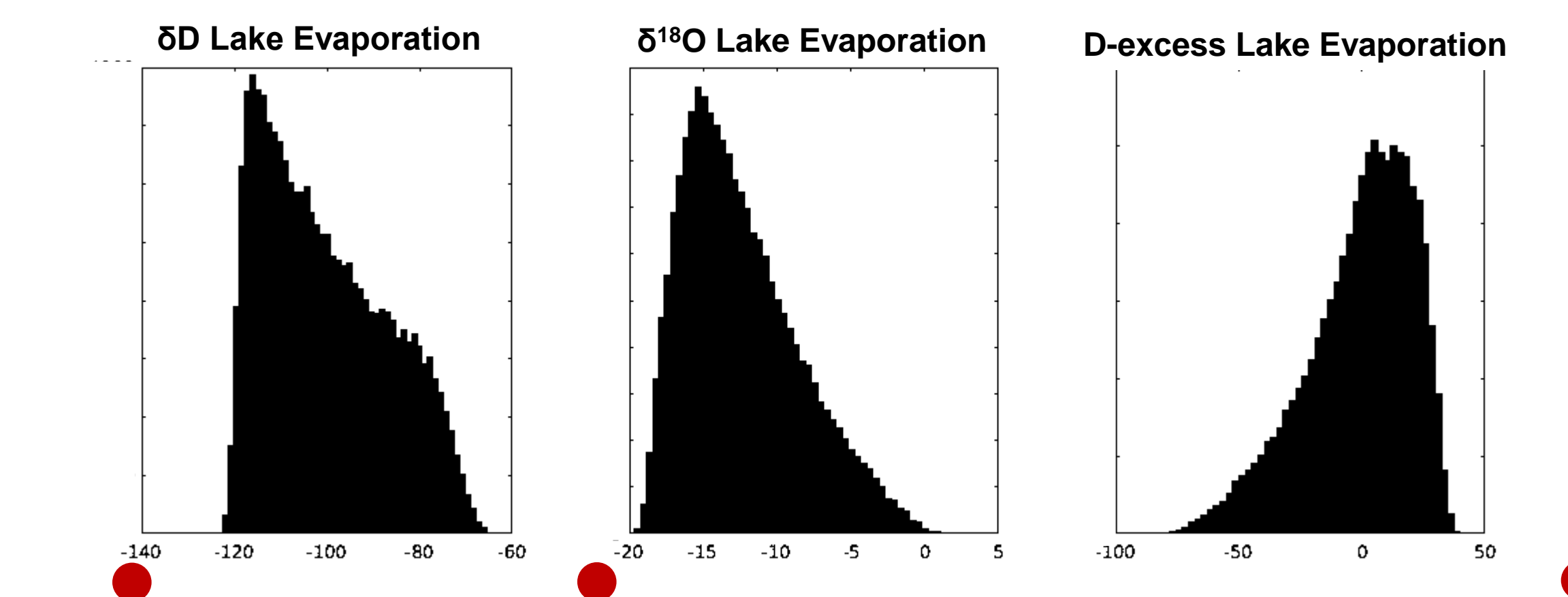


Figure 6. Craig and Gordon Monte Carlo simulations (histograms) are more enriched than a  $\delta_E$  Keeling Plot from observations around Lake Michigan (red dots) would suggest. This is the case in both  $\delta\text{D}$  and  $\delta^{18}\text{O}$  during both Flight 2 (a) and Flight 5(c). Flight 4 (b) Keeling Plot results fall within the range of the Monte Carlo experiment, and are included in the range of the Monte Carlo mean  $\pm$  sd.

## References

- Sharma, A. et al. (2018). *Earth's Future* 6, 1366–1379.
- Gat, J. R., Bowser, C. J. & Kendall, C. (1994). *Geophysical Research Letters* 21, 557–560.
- Xiao C, Lofgren BM, Wang J, Chu PY.(2016). *J Adv Model Earth Syst* 8:1969–1985.
- Xiao C, et al. (2018). *SCIENCE CHINA Earth Sciences*.
- Horita J, Rozanski K, Cohen S. (2008). *Isotopes in Environmental and Health Studies* 44:23–49.
- Merlivat L, Jouzel J.(1979). *Journal of Geophysical Research* 84:5029.
- Pataki DE, Ehleringer JR, Flanagan LB, et al. (2003). *Global Biogeochemical Cycles* 17.
- Flight Path images: NOAA © Google, Landsat/Copernicus

Funding was provided by a PCCRC Seed Grant. Thanks to our pilots. AM was supported by the National Science Foundation Graduate Research Fellowship Program under Grant No. (DGE-1333468r). Any opinions, findings, and conclusions or recommendations expressed in this material are those of the author(s) and do not necessarily reflect the views of the National Science Foundation.

